THE JOURNAL OF PHYSICAL CHEMISTRY

University of Texas Libraries

Subscriber access provided by University of Texas Libraries

Pronounced pressure effects on reversible electrode reactions in supercritical water

William M. Flarsheim, Allen J. Bard, and Keith P. Johnston

J. Phys. Chem., **1989**, 93 (10), 4234-4242 • DOI: 10.1021/j100347a066

Downloaded from http://pubs.acs.org on January 30, 2009

More About This Article

The permalink http://dx.doi.org/10.1021/j100347a066 provides access to:

- Links to articles and content related to this article
- Copyright permission to reproduce figures and/or text from this article

ACS Publications
High quality. High impact.

The Journal of Physical Chemistry is published by the American Chemical Society. 1155 Sixteenth Street N.W., Washington, DC 20036

rather by the specific organization of the neighbors.

The spectral shifts shown in Figures 8 and 9, and those of the absorption spectra, are qualitatively reversible. As previously mentioned, heating the porphyrin causes a decrease in Φ_f, and heating to the isotropic liquid phase causes some coalescence of the films. Furthermore, after cooling, the porphyrin is more ordered, with its attendant spectral shifts, than upon first warming.

Conclusions

Increasing the order of zinc octaalkylporphyrin thin films leads to characteristic changes in the absorption spectra that, for all but the most highly ordered films, can be explained on the basis of the molecular exciton model. The fluorescence quenching commonly seen in porphyrin thin films relative to the monomer in solution is shown to be a result of disorder. In ordered films, the fluorescence quantum yield, Φ_f, becomes comparable to the Φ_f in solution. In the most highly crystalline sample (the capillary-filled cell), the B band is broadened, the Q(0, 0) band is weakened and blue-shifted, and the Stokes shift is increased relative to the most ordered spin-coated film. Thus, several trends seen upon ordering of the spin-coated thin films are reversed. This reversal coincides with the appearance of a wavelength-dependent fluorescence quantum yield that decreases with increasing energy of excitation. This suggests that ring-to-ring charge-transfer-state formation may compete with fluorescence in the most highly crystalline samples. The photophysical properties of the pure liquid porphyrins show that the spectral shifts seen in these thin films are a function of the organization, not merely the proximity, of the neighboring chromophores.

Acknowledgment. We are grateful to the National Science Foundation for support of the Materials Research Group at the University of Texas under whose aegis this work was performed. We also thank Professor Steven E. Webber for his helpful comments on the manuscript.

Registry No. ZnOOEP, 119567-75-8; ZnOEP, 17632-18-7.

Pronounced Pressure Effects on Reversible Electrode Reactions in Supercritical Water

William M. Flarsheim,[†] Allen J. Bard,[‡] and Keith P. Johnston*,[†]

Departments of Chemical Engineering and Chemistry, The University of Texas, Austin, Texas 78712
(Received: August 22, 1988)

An alumina electrochemical cell containing an ultramicroelectrode was used to make precise voltammetric measurements in supercritical water. The effect of pressure on the redox potential of the I_2/I^- couple was measured from 230 to 300 bar at 385 °C. The partial molar volume change for the reduction of I_2 to I^-, $\Delta\bar{v}_{rxn}$, is pronounced, mostly because of the interplay between strong electrostatic forces and the large isothermal compressibility of the fluid. A modified Born model together with a perturbed hard sphere equation of state predicts the data accurately above 265 bar with no adjustable parameters. At lower pressures, ion pairing is thought to reduce the magnitude of $\Delta\bar{v}_{rxn}$. These large pressure effects on solvation free energies may be used to manipulate reaction equilibria and reaction mechanisms in supercritical water.

Introduction

A unique and useful feature of a supercritical fluid solvent is the pronounced effect of pressure on density and density-dependent properties such as the chemical potential of a solute. For example, the partial molar volume, that is $\partial\mu_i/\partial P$, of naphthalene at infinite dilution in supercritical ethylene is thousands of cm^3/mol negative because of the large compressibility of the solvent.[1] Partial molar volumes would be expected to be even more extreme in water due to the much larger change in the dielectric constant with pressure, and in the case of an ionic solute, to the strength of electrostatic forces. The objective of this work is to measure partial molar volume changes of reaction ($\Delta\bar{v}_{rxn}$) in supercritical water and to analyze the data theoretically in terms of pressure effects on solvation free energies and structures. The effects of both the ionic and nonionic intermolecular interactions will be analyzed independently to provide a fundamental understanding of solvation in expanded water. This is the first study to explore quantitatively the effect of pressure on redox potentials in supercritical water. A comparison between theory and experiment will be used to explain large pressure effects on reversible electrode reactions.

Previously, we performed electrochemical techniques such as voltammetry and chronoamperometry in supercritical water at extreme temperatures and pressures up to 400 K and 240 bar, respectively.[2] Electrochemical potentials and kinetic parameters for redox reactions of both inorganic and organic species were investigated from room temperature up to 400 K at a given pressure of 240 bar. The measured diffusion coefficients of iodide ion and hydroquinone were described quantitatively by the Stokes–Einstein theory. Several other recent studies have considered the use of near-critical and supercritical fluid solvents as a medium to manipulate electrochemical reactions.[3-5]

Thermodynamic data on electrolytes, and solutes in general, in near-critical and supercritical water (T_c = 373.9 °C; P_c = 220.5 bar; v_c = 324.4 kg/m^3) are important for a number of scientific and industrial areas including mineral geology and the formation of ore deposits, corrosion and scaling in electric power boilers, oxidation of waste in supercritical water, hydrothermal materials processing, and processes for coal and oil upgrading. Early measurements in supercritical water were primarily of the vapor pressures and phase compositions of electrolyte solutions.[6,7] Current investigations include electrochemical studies of metal corrosion,[8-10] measurement of ionic conductances,[11,12] and the

[†] Department of Chemical Engineering.
[‡] Department of Chemistry.

(1) Eckert, C. A.; Ziger, D. H.; Johnston, K. P.; Kim, S. *J. Phys. Chem.* **1986**, *90*, 2738.
(2) Flarsheim, W. M.; Tsou, Y.; Trachtenberg, I.; Johnston, K. P.; Bard, A. J. *J. Phys. Chem.* **1986**, *90*, 3857.
(3) Crooks, R. M. Ph.D. Dissertation, University of Texas at Austin, 1987.
(4) Flarsheim, W. M.; Johnston, K. P.; Bard, A. J. *J. Electrochem. Soc.* **1988**, *135*, 1939.
(5) Dombro, R. A.; Prentice, G. A.; McHugh, M. A. *J. Electrochem. Soc.* **1988**, *135*, 2219.
(6) Keevil, N. B. *J. Am. Chem. Soc.* 1942, *64*, 841.
(7) Sourirajan, S.; Kennedy, G. C. *Am. J. Sci.* **1962**, *260*, 115.
(8) Macdonald, D. D. The Electrochemistry of Metals in Aqueous Systems at Elevated Temperatures. In *Modern Aspects of Electrochemistry, Vol. 11*; Bockris, J. O'M., Conway, B. E., Eds.; Plenum Press: New York, 1975; Chapter 4.
(9) Macdonald, D. D. *Corrosion* **1978**, *34*, 75.
(10) Macdonald, D. D.; Scott, A. C.; Wentreck, P. *J. Electrochem. Soc.* **1981**, *128*, 250.
(11) Marshall, W. L. *Pure Appl. Chem.* **1985**, *57*, 283.

0022-3654/89/2093-4234$01.50/0 © 1989 American Chemical Society

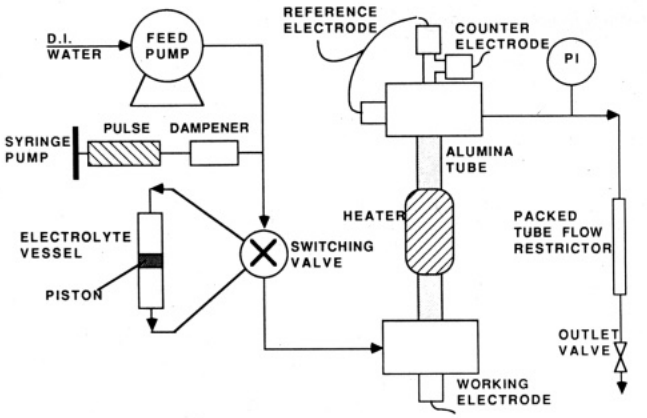

Figure 1. Schematic of equipment for electrochemistry in supercritical water.

phase behavior of many light gases in supercritical water and NaCl solutions.[13,14] In addition, the solvation energy, partial molar heat capacity, and partial molar volume of many electrolytes have been measured to temperatures above 300 °C,[15-21] though not above the critical temperature of water.

This study is part of a broad effort to understand pressure effects on properties of solutes and on chemical reaction rates and equilibria in supercritical fluid solvents. The simplest pressure-dependent property is the partial molar volume of a solute, which was discussed above. The activation volume, which is obtained from the slope of a rate constant with pressure, was measured for the thermal decomposition of α-chlorobenzyl methyl ether in supercritical fluid 1,1-difluoroethane.[22] At 403 K, it reaches -6000 cm^3/mol where the compressibility is a maximum. This value is 2 orders of magnitude greater than those observed in liquid solvents and an order of magnitude greater than any previously reported value in an inert solvent. The present paper extends the scope to include an ionic reactant and a much more polar supercritical fluid, water. An interesting and useful property of supercritical water is that the pressure may be varied to change mechanisms from free radical to ionic[23] or from pyrolysis to solvolysis.[24] This study of pressure effects on the stability of ions and molecules undergoing reaction is important for understanding these mechanism changes.

The working electrode that was used for a previous study in supercritical water[2] was unsuitable for making extremely accurate measurements of redox potentials. The relatively large size of the working electrode led to large iR potential drops in the cell, especially above the critical temperature where the solution resistance is high. By use of an ultramicroelectrode[25,26] of 25-μm diameter, with an area of 5×10^{-6} cm^2, which is smaller by a factor of 400 than that of the electrode previously employed, potentials could be measured to ±4 mV. In addition, a small high-pressure mercury/mercury sulfate electrode was built to provide a stable reference potential for these measurements.

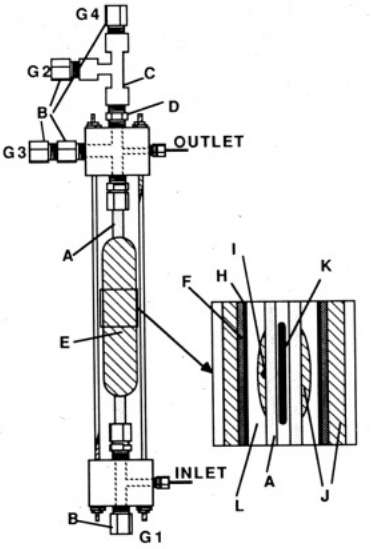

Figure 2. High-temperature, high-pressure electrochemical cell: A, 0.635 cm ($^1/_4$-in.) o.d. × 0.238 cm ($^3/_{32}$-in.) i.d. × 15 cm (6-in.) long alumina tube (99.8% Al_2O_3); B, stainless steel (SS) adaptors; C, SS tee; D, SS adaptor; E, brass heater assembly; F, nichrome heating coil; G, $^1/_8$-in. NPT electrode ports, G1, working, G2, counter, G3, reference, G4, platinum reference wire; H, brass tube; I, type J thermocouple; J, fiberglass insulation; K, location of working and reference electrodes in the cell; L, air gap.

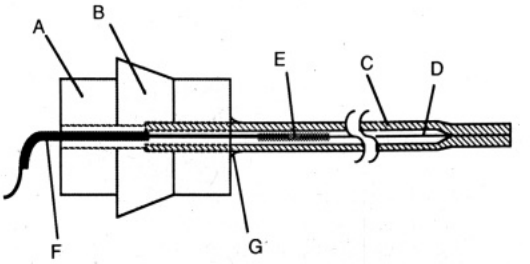

Figure 3. High-pressure electrode fitting and platinum microelectrode: A, 0.635 cm ($^1/_4$-in.) diameter aluminum rod; B, aluminum ferrule; C, 0.2-cm Pyrex tube; D, 25-μm platinum wire; E, electrical solder; F, wire lead; G, epoxy seal. This assembly is mounted in a $^1/_4$-in. tube to a $^1/_8$-in. NPT stainless steel Swagelok fitting.

Experimental Section

Equipment and Electrodes. The experimental apparatus was similar to a previous design,[2] with several modifications as shown in Figures 1 and 2. The important advantages of the design are that the alumina reaction cell was inert, insoluble, and small in volume so that the contents of the tube and the temperature could be changed quickly. Another advantage of the small volume was that the safety shield was not damaged if a tube burst. Only the central section of the tube was heated so that the pressure seals at the ends were cool. A 60-cm^3 syringe pump (High Pressure Generator Model No. 87-6-5, High Pressure Equipment Co., Inc., Erie, PA) was used in addition to the feed pump so that the pressure could be increased or decreased with minimal amounts of displacement of solution in the alumina reaction cell. As a result of this design, thermal equilibrium was achieved in about 3 min after each new value of pressure was selected.

The high-pressure electrode seal, shown in Figure 3, was used in constructing both the working and reference electrodes. A hole smaller than the glass tube, but large enough to accommodate the wire lead, was drilled through a 1.9-cm ($^3/_4$ in.) length of 0.635 cm ($^1/_4$ in.) diameter aluminum rod. One end of the hole was widened to the diameter of the glass tube and a depth of 0.95 cm ($^3/_8$ in.). The glass was sealed to the aluminum with epoxy. Finally, the aluminum was mounted in a $^1/_4$-in. tube to $^1/_8$-in.

(12) Marshall, W. L. *J. Chem. Eng. Data* **1987**, *32*, 221.
(13) Franck, E. U. *Pure Appl. Chem.* **1985**, *57*, 1065.
(14) Franck, E. U. *Pure Appl. Chem.* **1987**, *59*, 25.
(15) Cobble, J. W.; Murray, R. C., Jr. *Discuss. Faraday Soc.* **1977**, *64*, 144.
(16) Wood, R. H.; Smith-Magowan, D.; Pitzer, K. S.; Rogers, P. S. Z. *J. Phys. Chem.* **1983**, *87*, 3297.
(17) Gates, J. A.; Tillett, D. M.; White, D. E.; Wood, R. H. *J. Chem. Thermodyn.* **1987**, *19*, 131.
(18) White, D. E.; Doberstein, A. L.; Gates, J. A.; Tillett, D. M.; Wood, R. H. *J. Chem. Thermodyn.* **1987**, *19*, 251.
(19) White, D. E.; Gates, J. A.; Wood, R. H. *J. Chem. Thermodyn.* **1987**, *19*, 493.
(20) White, D. E.; Ryan, M. A.; Cavalucci Armstrong, M. A.; Gates, J. A.; Wood, R. H. *J. Chem. Thermodyn.* **1987**, *19*, 1023.
(21) White, D. E.; Gates, J. A.; Wood, R. H. *J. Chem. Thermodyn.* **1987**, *19*, 1037.
(22) Johnston, K. P.; Haynes, C. *AIChE J.* **1987**, *33*, 2017.
(23) Antal, M. J.; Brittain, A.; DeAlmeida, C.; Ramayya, S.; Roy, J. C. *ACS Symp. Ser.* **1986**, *No. 329*, 77.
(24) Abraham, M. A.; Klein, M. T. *Ind. Eng. Chem. Prod. Res. Dev.* **1985**, *24*, 300.
(25) Howell, J. O.; Wightman, R. M. *Anal. Chem.* **1984**, *56*, 524.
(26) Bond, A. M.; Fleischmann, M.; Robinson, J. *J. Electroanal. Chem.* **1984**, *168*, 299.

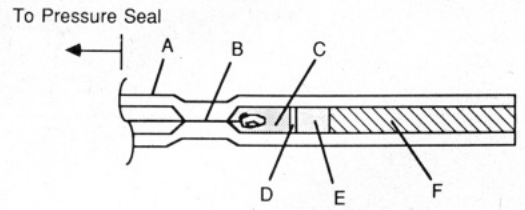

Figure 4. Mercury/mercurous sulfate reference electrode: A, 0.3-cm Pyrex tube; B, 50-μm platinum wire; C, mercury; D, mercurous sulfate; E, potassium sulfate; F, glass wool. This electrode uses the same pressure seal shown in Figure 3.

NPT 316 stainless steel Swagelok fitting by using aluminum ferrules.

All measurements were made with a 25-μm platinum-wire-in-glass ultramicroelectrode (UME). First, a 25-μm platinum wire (99.95% Pt from the AESAR division of Johnson Matthey) was sealed in the end of a 0.2-cm Pyrex tube. The method for doing this is described elsewhere.[3,4] The electrode was sanded with 600-grit sandpaper and polished with 1-μm diamond paste. The electrode was oxidized at about 40 V in 9 M sulfuric acid to clean the electrode surface, which gave it a reproducible activity.

A mercury/mercurous sulfate reference electrode in a cool region of the cell was connected directly to a 50-μm platinum-in-glass electrode in the hot zone, in a dual reference electrode design.[27] The pressure seal in the reference electrode was the same as that in the working electrode. A diagram of the reference electrode is shown in Figure 4. The mercury/mercurous sulfate electrode establishes the potential of the platinum electrode, without any significant potential difference. The purpose of the platinum wire is to reduce the effective solution resistance between the working and reference electrodes, to reduce the *iR* drop.

Procedure. Reagent grade sulfuric acid was recrystallized as the monohydrate,[28] to prepare 0.1 M stock solutions. All other chemicals were of reagent grade and used as received. Fresh potassium iodide solutions were prepared daily by using distilled water that was further treated with a Millipore, Milli-Q reagent water system. All experiments were conducted in solutions that had been deaerated with nitrogen.

The cyclic voltammograms (CV's) were obtained at each pressure after allowing about 3 min to reach thermal equilibrium. Measurements were made as quickly as possible so that during a run thermal diffusion would not affect the composition of the solution in the hot zone and so that as many data as possible could be taken before the cell burst. The alumina tubes burst in minutes to hours at high temperature and pressure. The cyclic voltammetry was performed by using a Princeton Applied Research Model 173/176 potentiostat with a Model 175 universal programmer. No positive feedback resistance compensation was used with the potentiostat, since this would sometimes cause the potentiostat to overload and damage the electrodes. Instead, positive feedback was added digitally after the scans had been recorded. The resistance compensation procedure is explained below.[29]

All CV's used for determining the redox potential of the I_2/I^- couple were made at 200 V/s. This high speed was used so that diffusion would be linear (edge effects on the UME would be negligible) and the redox potential could be determined by averaging the anodic and cathodic peak potentials. The current and potential data were recorded by using a Norland Model 3001 digital oscilloscope with a signal averager. A total of 100 voltage cycles were averaged to produce each of the cyclic voltammograms used for measuring redox potential.

Digital Processing of Cyclic Voltammograms. The averaged cyclic voltammograms were stored on floppy disks and then were processed with a Norland digital oscilloscope. These CV's were

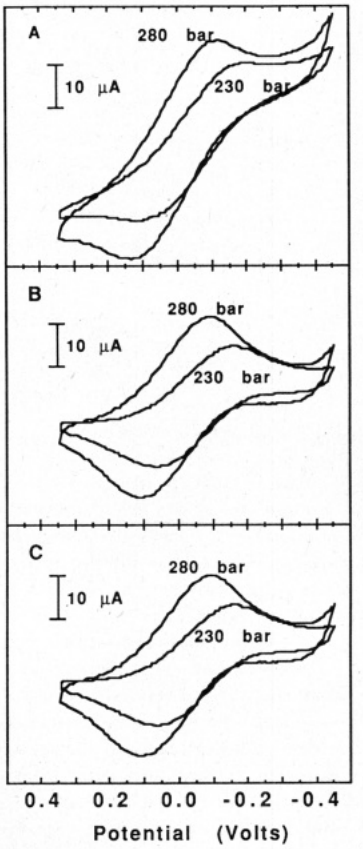

Figure 5. Digital processing of high-temperature cyclic voltammograms: solution, 7.6 mM KI in 0.1 M H_2SO_4; electrode area, 5×10^{-6} cm^2; scan rate, 200 V/s; temperature, 385 °C. (A) Unprocessed cyclic voltammograms. (B) Voltammograms corrected for charging current. (C) Voltammograms corrected for solution *iR* drop by using positive current feedback and for charging current.

distorted from the ideal Nernstian shape by the voltage drop due to the current, both faradaic and charging, passing through the uncompensated cell resistance, R_u. Figure 5A shows typical cyclic voltammograms at 230 and 280 bar. The CV's are sloped even at potentials where no electrochemical reaction occurs due to the charging current. To correct for this, the slope of the current in front of the I^- oxidation wave, where there is no faradaic current, was determined with the oscilloscope and then subtracted, giving the CV's shown in Figure 5B. (Specifically, at each data point in the region in front of the oxidation wave, the average slope across the next 10 data points, which covers 20 mV, was determined.) The minimum slope found in this region was used to calculate the charging current correction. This correction, which assumes a double-layer capacitance independent of potential in the region of the wave, produced a flat base line in the cyclic voltammogram, so that more accurate peak potentials could be determined.

The peak separation in these cyclic voltammograms is greater than the Nernstian value of $2.3RT/nF$ (131 mV at 385 °C). The I_2/I^- couple has been found to be reversible in acid media,[30] so the excess peak separation is due to solution resistance. This is eliminated digitally by adding positive current feedback to the recorded voltage, which achieves the same effect as using positive feedback compensation on the potentiostat.[29] The resulting CV's are shown in Figure 5C. The amount of feedback added was usually equivalent to a R_u of 8–20 kΩ, with the higher values found at lower pressures. In a separate measurement of the cell resistance at 385 °C and 250 bar, a value of 17 kΩ was obtained. For each series of redox measurements, the amount of background subtraction and positive feedback added was similar for each CV, so the actual effect on the measurement of redox shifts with pressure was very small. After the above corrections were per-

(27) Hermann, C. C.; Perrault, G. G.; Pilla, A. A. *Anal. Chem.* **1968**, *40*, 1173.

(28) Perrin, D. D.; Armarego, W. L. F.; Perrin, D. R. *Purification of Laboratory Chemicals*, 2nd. ed.; Pergamon Press: New York, 1980.

(29) Flarsheim, W. M. Ph.D. Dissertation, University of Texas at Austin, 1988.

(30) Kolthoff, I. M.; Jordan, J. *J. Am. Chem. Soc.* **1953**, *75*, 1571.

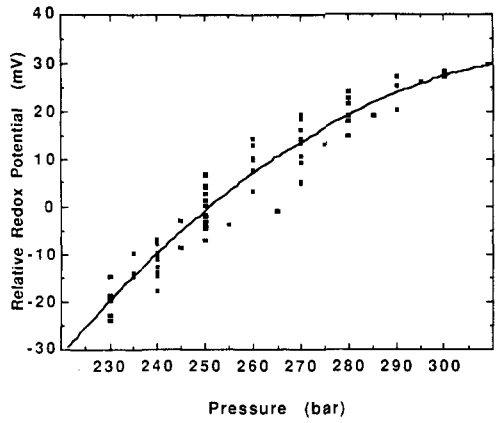

Figure 6. Normalized redox potential of the I_2/I^- couple measured in 0.1 M H_2SO_4 at 385 °C.

formed on each cyclic voltammogram, the anodic and cathodic peak potentials of the I_2/I^- wave were measured and averaged to give the redox potential.

Results and Discussion

Sulfuric Acid Solution. The goal of these experiments was to demonstrate the existence of large changes in the redox potential of an electroactive species as a function of pressure in supercritical water. This measurement is complicated by the fact that a reference electrode has not yet been designed for use above the critical point of water. Very few reference systems have been developed for use above 250 °C.[9,31,32] A reference electrode in the cool zone, maintained at 25 °C, was used for this work. A change in cell pressure had a negligible effect on the potential of the reference electrode because its components are essentially incompressible at 25 °C. The drawback of using a room-temperature reference electrode is that it introduces an unknown thermal liquid junction potential ($\Delta\phi_{TLJP}$) into the redox measurements. The pressure dependence of the $\Delta\phi_{TLJP}$ redox was estimated experimentally, as will be explained in detail, so that the pressure derivative of the iodine redox potential ($\partial E_{I_2/I^-}/\partial P$) could also be determined.

The redox potential of the I_2/I^- couple was measured by cyclic voltammetry at 385 °C over the pressure range 230–300 bar. At lower pressures, the solution resistance was too high to measure potentials accurately. The electrolyte solutions contained between 7.2 and 7.6 mM KI with 0.1 M H_2SO_4 as the supporting electrolyte. The critical temperature of a 0.1 M H_2SO_4 solution is 380 °C,[33] so the solutions were supercritical and near the maximum compressibility. The data obtained from three experimental runs are plotted in Figure 6. The potential scale has been normalized so that at 250 bar the average potential is zero. This adjustment corrects for the small changes in the reference potential from day to day. Since determination of the slope of the data is the primary objective, the absolute potential scale is not important. The unnormalized data from the experimental runs are tabulated elsewhere.[29]

The data were fit by least squares to a quadratic equation of the form

$$E_{redox} = aP^2 + bP + c \quad (1)$$

where E is in millivolts and P in bar. The values of the constants are $a = -0.0055$, $b = 3.60$, and $c = -556$, and the correlation coefficient $R^2 = 0.918$. A higher order polynomial would not be appropriate because of the uncertainty in the data. To relate this result to thermodynamic models, it is convenient to convert from potential to energy units. The electrochemical half-reaction for reduction is

$$\tfrac{1}{2}I_2 + e^- \rightleftharpoons I^- \quad (2)$$

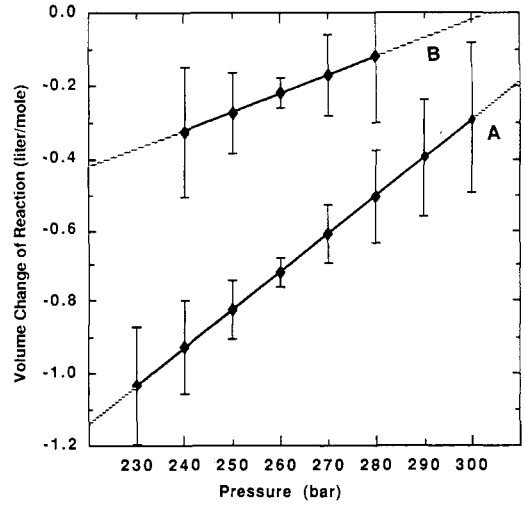

Figure 7. $\Delta\bar{v}$ for the reduction of $1/2I_2$ at 385 °C including the contribution from the thermal liquid junction potential: A, electrolyte, 0.1 M H_2SO_4; B, electrolyte, 0.08 M $KHSO_4$ plus 0.02 M H_2SO_4.

The pressure derivative of the free energy change of this reaction is given by

$$\Delta\bar{v}_{rxn}\ (cm^3/mol) = -nF(\partial E/\partial P) = 10.6P - 3470 \quad (3)$$

where n is the number of electrons, in this case 1, and F is the Faraday constant. This result contains a contribution from the pressure derivative of the thermal liquid junction potential ($\partial\Delta\phi_{TLJP}/\partial P$), which is addressed in the next section.

The partial molar volume change for this reaction is

$$\Delta\bar{v}_{rxn} = \bar{v}_{I^-} - \tfrac{1}{2}\bar{v}_{I_2} \quad (4)$$

since the partial molar volume of an electron is negligible. At 385 °C, $\Delta\bar{v}_{rxn}$ varies from −1030 cm^3/mol at 230 bar to −290 cm^3/mol at 300 bar (see Figure 7). This implies that the partial molar volume of I^- must be much more negative than that of I_2. Measurements in other supercritical fluids have shown that most solutes have large negative partial molar volumes at low concentrations; for example at 308.5 K and 79.8 bar, the partial molar volume of naphthalene in supercritical fluid carbon dioxide at infinite dilution is −7800 cm^3/mol.[1] The electrostatic attraction between iodide ions and water dipoles produces a significant clustering of water molecules around the ion and gives rise to a very negative partial molar volume. This model is discussed more fully in a later section.

Thermal Liquid Junction Potential. When a temperature gradient is imposed on an electrolyte solution, the positive and negative ions will begin to diffuse at rates that depend upon the chemical potential gradient and the transport properties of the individual ionic species. For the simplest case of only two ionic species, there is no physical reason for the two initial fluxes to be equal. The unequal fluxes disturb the electroneutrality of the solution. In a few nanoseconds, the redistribution of charge sets up a potential gradient that opposes the unequal diffusion rates.[34] This potential, known as the thermal liquid junction potential ($\Delta\phi_{TLJP}$), keeps the separate ionic fluxes equal and preserves electroneutrality in the solution. Standard treatments of the theory of the $\Delta\phi_{TLJP}$ consider it to be a function of the temperature gradient and the solution properties of ionic species; no mention is made of a pressure dependence of $\Delta\phi_{TLJP}$. There have been few measurements of the $\Delta\phi_{TLJP}$ above 100 °C,[35] so it would be inappropriate to assume that the pressure effect is insignificant in the compressible critical region.

The measured value of the redox potential versus the potential of the low-temperature reference electrode is the sum of the redox

(31) Niedrach, L. W. *Angew. Chem., Int. Ed. Engl.* **1987**, *26*, 161.
(32) Hettiarachchi, S.; Macdonald, D. D. *J. Electrochem. Soc.* **1987**, *134*, 1307.
(33) Marshall, W. L.; Jones, E. V. *J. Inorg. Nucl. Chem.* **1974**, *36*, 2313.
(34) Home, F. H.; Borey, B. K. *Int. J. Thermophys.* **1986**, *7*, 87.
(35) Macdonald, D. D.; Scott, A. C.; Wentrcek, P. *J. Electrochem. Soc.* **1979**, *126*, 1618.

potential at the actual reaction temperature plus the thermal liquid junction potential

$$E = E_{rxn} + \Delta\phi_{TLJP} \quad (5)$$

In order to analyze pressure variations of the redox potential, it is necessary to investigate the pressure derivative of the thermal liquid junction potential, as is evident from the equation

$$\frac{\partial E_{rxn}}{\partial P} = \frac{\partial E}{\partial P} - \frac{\partial \Delta\phi_{TLJP}}{\partial P} \quad (6)$$

The term $\partial\Delta\phi_{TLJP}/\partial P$ may be either positive or negative depending on the supporting electrolyte. The prediction of the sign of $\partial\Delta\phi_{TLJP}/\partial P$, based on the limited experimental data concerning thermal liquid junction potentials in the literature, is discussed in the Appendix. By measurement of $\partial E/\partial P$ in two different supporting electrolytes, for which the signs $\partial\Delta\phi_{TLJP}/\partial P$ are opposite, it is possible to determine an upper and lower bound on the actual $\partial E_{rxn}/\partial P$.

The data presented above were obtained with 0.1 M H_2SO_4 as the supporting electrolyte. The derivative $\partial\Delta\phi_{TLJP}/\partial T$ for acid solutions is negative, implying that $\partial\Delta\phi_{TLJP}/\partial P$ is positive (see Appendix), and therefore the values of $\partial E/\partial P$ are higher than $\partial E_{rxn}/\partial P$.

Potassium Bisulfate Solution. In order to put a lower bound on the value of $\partial E_{rxn}/\partial P$ for the I_2/I^- couple, it was necessary to make the measurement by using an electrolyte with a positive $\partial\Delta\phi_{TLJP}/\partial T$, which would imply a negative $\partial\Delta\phi_{TLJP}/\partial P$. One choice for an electrolyte would have been an alkali-metal halide such as KCl. The $\partial\Delta\phi_{TLJP}/\partial T$ of KCl and most alkali-metal halides is near zero at 25 °C, but becomes large and positive with increasing temperature.[35,36] Halides could not be used because the possible formation of multi-halide ions such as I_2Cl^- would affect the redox equilibrium. Instead, $KHSO_4$ was chosen as the major supporting electrolyte. At near-critical conditions, there is essentially no dissociation of the bisulfate ion (HSO_4^-),[37] so $KHSO_4$ may be considered a 1:1 electrolyte. $KHSO_4$ has the same critical temperature versus concentration dependence as KCl and other alkali-metal halides in supercritical water and has other similar properties.[33] Therefore, it is reasonable to assume that $\partial\Delta\phi_{TLJP}/\partial T$ for $KHSO_4$ is positive at high temperatures.

The actual electrolyte chosen for these measurements was 0.08 M $KHSO_4$ plus 0.02 M H_2SO_4. The acid was necessary to suppress the oxidation of I_2 to IO_3^-. The 4:1 ratio of $KHSO_4$ to H_2SO_4 is not indicative of the actual ratio of positive ions in the electrolyte. The pK_a of H_2SO_4 is about 2.8 at 385 °C and 300 bar and is smaller at lower pressures.[37] Since $KHSO_4$ dissociates almost completely, the HSO_4^- from $KHSO_4$ will suppress dissociation of H_2SO_4 so that the ratio of K^+ to H^+ is on the order of 200:1. Thus this supporting electrolyte can be considered to be predominantly $KHSO_4$ for purposes of estimating the thermal liquid junction potential.

The redox potential of the couple I_2/I^- was measured at 385 °C and at pressures from 240 to 280 bar in a solution containing 7.6 mM KI and the electrolyte described above (see Figure 8). As with the data taken in sulfuric acid, the potential scale has been normalized so that at 250 bar the average potential is zero. The unnormalized data are available elsewhere.[29]

A least-squares fit of these data using eq 1 gives $a = -0.0026$, $b = 1.59$, and $c = -232$ with a correlation coefficient $R^2 = 0.920$. The equation obtained for the pressure derivative may be expressed as a partial molar volume change of reaction, that is

$$\Delta\bar{v}_{rxn}\ (cm^3/mol) = 5.0P - 1530 \quad (7)$$

Estimation of $\Delta\bar{v}_{rxn}$. The two measurements of $\Delta\bar{v}$, in H_2SO_4 and $KHSO_4$, are plotted in Figure 7. From the analysis of the contribution of the thermal liquid junction potential to the measured $\partial E/\partial P$, it is reasonable to conclude that the true value of $\Delta\bar{v}_{rxn}$ lies between the two lines. In either case, there is a pronounced pressure effect on the redox potential for this reaction.

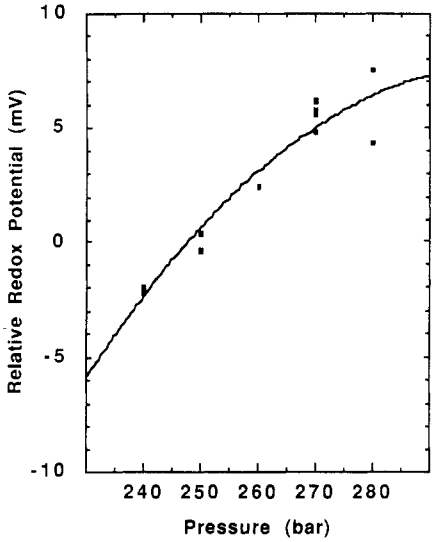

Figure 8. Normalized redox potential of the I_2/I^- couple measured in 0.08 M $KHSO_4$ plus 0.02 M H_2SO_4 at 385 °C.

Analysis

Basis of the Model. The $\Delta\bar{v}$ measurements presented here are the first ones reported for a reaction conducted near the critical point and involving an ionic species. These data provide a unique opportunity for examining models for ions, and solutes in general, in the critical region. Since the ionic and nonionic contributions to the chemical potential of a solute can be treated separately, the pressure derivative may be expressed as

$$\Delta\bar{v}_{rxn} = \bar{v}_{I^-}(\text{ionic}) + (\bar{v}_{I^-}(\text{nonionic}) - \tfrac{1}{2}\bar{v}_{I_2}) \quad (8)$$

The ionic contribution will be calculated by using a modification of the Born equation that takes into account the compressibility of water. A perturbed hard sphere equation of state will be used to treat the contribution due to nonionic interactions. Iodine, which is nonionic with a dipole moment of zero, interacts with water through a repulsive force, determined largely by molecular volume, and attractive dispersion and induction forces that are determined largely by molecular polarizability. The interaction between iodide ions and water is more complex because of ion–dipole forces which are long-range.

Nonionic Interactions. The partial molar volume of a component may be expressed as the product of two terms by using a triple product relationship

$$\bar{v}_i = v k_T n \left(\frac{\partial P}{\partial n_i}\right)_{T,v,n_j} \quad (9)$$

where v is the molar volume and k_T is the isothermal compressibility, $-1/v\ (\partial v/\partial P)$. Whereas k_T of the solvent is infinite at the critical point, the other derivative, $(\partial P/\partial n_i)$, remains finite at the critical point and varies much less than the compressibility in the critical region.[1] Equation 9 is the starting point for the evaluation of the nonionic repulsive and attractive parts of $\bar{v}_{I_2}$ and $\bar{v}_{I^-}$.

In the experiments, the total mole fraction of all solutes was less than 0.004, and the mole fractions of the two iodine species were smaller than this by an order of magnitude. These concentrations are sufficiently small such that the properties of pure water may be used to approximate k_T, while $(\partial P/\partial n_i)$ may be calculated at infinite dilution. The volumetric data for water were calculated from the equation of state developed by Haar et al.[38]

(36) Milazzo, G.; Sotto, M.; Devillez, C. *Z. Phys. Chem.* **1967**, *54*, 13.
(37) Quist, A. S.; Marshall, W. L.; Jolley, H. R. *J. Phys. Chem.* **1965**, *69*, 2726.

(38) Haar, L.; Gallagher, J. S.; Kell, G. S. *NBS/NRC Steam Tables: Thermodynamic and Transport Properties and Computer Programs for Vapor and Liquid States of Water in SI Units*; Hemisphere Publishing: New York, 1984.

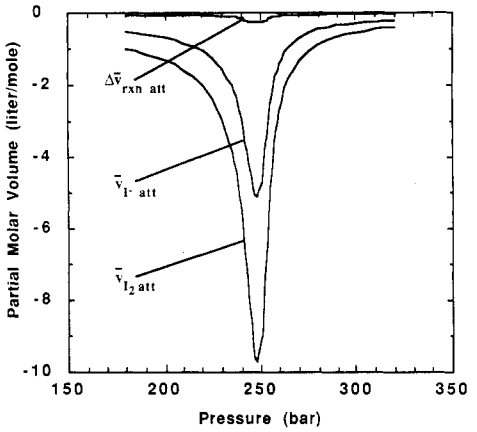

Figure 9. Contribution of nonionic attractive forces to $\Delta\bar{v}_{rxn}$ for the reduction of $1/2I_2$ at 385 °C.

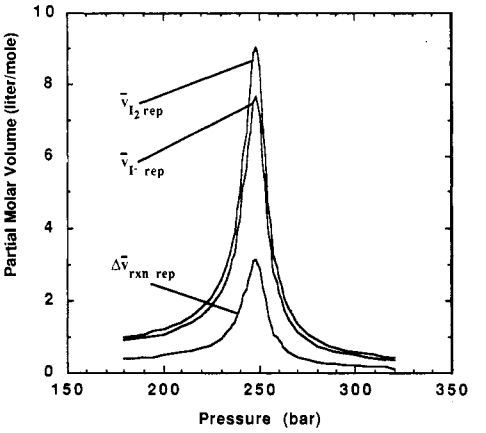

Figure 10. Contribution of nonionic repulsive forces to $\Delta\bar{v}_{rxn}$ for the reduction of $1/2I_2$ at 385 °C.

The Carnahan-Starling–van der Waals (CS–VDW) equation of state was used to calculate the derivative $(\partial P/\partial n_2)^\infty$, where 2 refers to the solute, since it includes an accurate repulsive term and since it has been tested widely.[39] The resulting expression is

$$n\left(\frac{\partial P}{\partial n_2}\right)^{\infty}_{T,V,n_j} = \frac{RT}{v}\frac{(1+y+y^2-y^3)}{(1-y)^3} + \frac{RTb_2}{4v^2}\frac{(4+4y-2y^2)}{(1-y)^4} - \frac{2a_{12}}{v^2} \quad (10)$$

where $y = b/4v$, b is the mixture volume parameter which at infinite dilution is b_1, which is the size parameter for water, b_2 is the size parameter for the solute, and a_{12} is the mean attractive parameter calculated from the van der Waals mixing rule $a_{12} = (a_1a_2)^{1/2}$. The first two terms in the equation account for repulsive forces, while the last term represents the attractive interaction. The parameters a_i and b_i were calculated from T_c and P_c for H_2O and I_2.[29] The critical properties of xenon were used to calculate a_{I^-} and b_{I^-}.

The calculated values of the attractive and repulsive nonionic contributions to the partial molar volume are shown in Figures 9 and 10, respectively. As can be seen in Figure 9, the stoichiometry of the reaction is such that the nonionic attractive contributions of $\bar{v}_{I_2}$ and $\bar{v}_{I^-}$ roughly cancel (see eq 8). The nonpolar attractive interactions for two I^- atoms with the solvent are about the same as for one I_2 molecule, so that the attractive contribution to $\Delta\bar{v}_{rxn}$ is small. The effect of the repulsive forces is quite different, as shown in Figure 10. The volume of two iodide ions is much greater than the molecular volume of I_2, so that the repulsive contribution to $\Delta\bar{v}_{rxn}$ is largely positive. The total nonionic contribution to $\Delta\bar{v}_{rxn}$ is positive, since it is dominated by the repulsive term as shown in Figure 11, while the experimental $\Delta\bar{v}_{rxn}$ is negative. This indicates clearly that the contribution from the electrostatic interaction of I^- with water is greater than the nonionic contribution. The shapes of the curves in Figures 9 and 10 resemble that of the isothermal compressibility, because of the relationship in eq 9.[1] The maximum in the isothermal compressibility and thus the $\Delta\bar{v}$ values is at a pressure slightly above P_c since the temperature is above T_c.

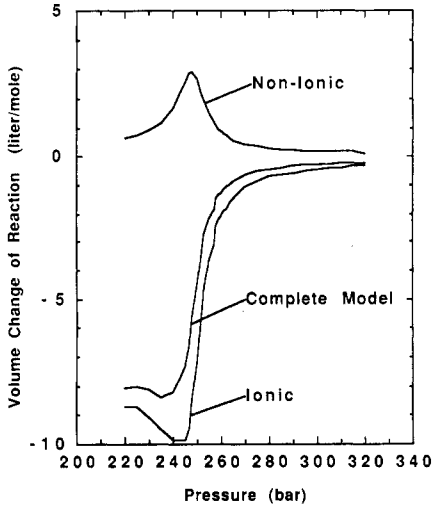

Figure 11. Prediction of the modified Born–perturbed hard sphere model for the reduction of $1/2I_2$ at 385 °C.

Modified Born Equation. The classical Born equation for the Gibbs energy of transferring an ion from vacuum to a medium of dielectric constant ϵ is

$$\Delta G_{solv} = -\frac{q^2}{8\pi\epsilon_0 r}\left(1 - \frac{1}{\epsilon}\right) \quad (11)$$

where q and r are the charge and radius of the ion, respectively.[40] Here we focus on the second term, the free energy required to create a charged ion in a dielectric medium, which may be considered to be the ionic part of the chemical potential

$$\mu_i(\text{ionic}) = \frac{q^2}{8\pi\epsilon_0\epsilon r} \quad (12)$$

Born used the ionic crystal radii for r, but other values have been suggested.[41] The Born equation assumes that the dielectric constant of the solvent is equal to the bulk value even close to the ion where the electric field is strong. This assumption is much more reasonable for a relatively incompressible liquid than for a highly compressible supercritical fluid. The electric field near an ion attracts strongly the surrounding fluid, which gives rise to an increase in the local density and thus the local dielectric constant. The result is a lower μ_i(ionic), since the ion is stabilized to a greater extent than that which is predicted by the Born equation.

The Born equation has been modified by Wood et al.[42] to include the effects due to the compressibility of the solvent. The derivation is based on earlier work by Frank on the thermodynamics of a fluid substance in an electric field.[43] The derivation begins with an expression for the change in density with the imposition of an electric field at constant chemical potential and temperature:[42]

$$\frac{d\rho}{\rho^2} = \frac{\epsilon_0 k_T}{2}\left(\frac{\partial\epsilon}{\partial\rho}\right)_{E,T} dE^2 \quad (13)$$

(39) Carnahan, N. F.; Starling, K. E. *AIChE J.* **1972**, *18*, 1184.

(40) Born, M. *Z. Phys.* **1920**, *1*, 45.
(41) Rashin, A. A.; Honig, B. *J. Phys. Chem.* **1985**, *89*, 5588.
(42) Wood, R. H.; Quint, J. R.; Grolier, J. P. E. *J. Phys. Chem.* **1981**, *85*, 3944.
(43) Frank, H. S. *J. Chem. Phys.* **1955**, *23*, 2023.

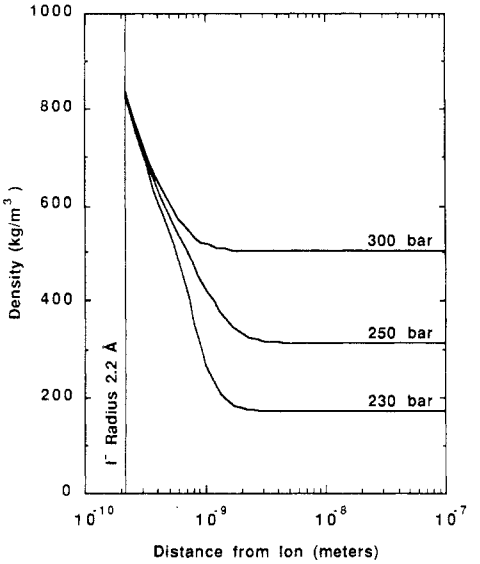

Figure 12. Variation of local density with distance from a univalent ion in water at 385 °C.

The electrostatic work is the product of the field times the degree to which the element is polarized:

$$\omega_e' = \int_0^E \epsilon_0 E \, \mathrm{d}\left[\frac{(\epsilon - 1)E}{\rho}\right] \tag{14}$$

The total free energy required to charge an ion is given by a term that describes the energy for polarization of the fluid, along with a second term for the energy required to establish the field in space[42]

$$\mu_i(\text{ionic}) = \int_a^\infty \left(\omega_e'\rho + \frac{\epsilon_0 E^2}{2}\right) 4\pi r^2 \, \mathrm{d}r \tag{15}$$

The relation between the electric field and the distance from the ion is

$$E = q/(4\pi\epsilon_0\epsilon r^2) \tag{16}$$

Equation 15 is integrated numerically with density as the independent variable. The bulk density is incremented by a small value $d\rho$. This information is used to determine the electric field strength at the new density from eq 13, and the distance from the ion by using eq 16. Finally, the polarization work integral (eq 14) is evaluated and used in eq 15. Equation 15 becomes the classical Born equation in the limit where ϵ and ρ are independent of the field.

Ionic Contribution to the Partial Molar Volume of I$^-$. The modified Born model was used to calculate the ionic contribution to the partial molar volume of I^-, $\bar{v}_{I^-}$(ionic). The necessary *PVT* data for water were calculated by using Fortran subroutines from Haar et al.,[38] and the dielectric constant was calculated from the equation of Uematsu and Franck.[44] For I^-, the ionic crystal radius of 2.2 Å was used as the lower limit of integration.

The theory may be used to examine the value of the local solution density and μ_i(ionic) as a function of radius. Figure 12 shows the local density around an ion as a function of radius for three pressures at which experimental data were also measured. There is a large degree of clustering of solvent about the ion at 230 bar as the local density exceeds the bulk value by a factor of up to 4. A novel and interesting result is that the local densities approach each other near the ion ($R < 4$ Å) for this pressure range, even though the bulk densities differ by a factor of 3. This observation may be explained more effectively by using a plot of local density versus pressure. In Figure 13, the local density was defined at a radius of 2.2 Å; similar results would be obtained if the radius were chosen to be slightly larger. The local density

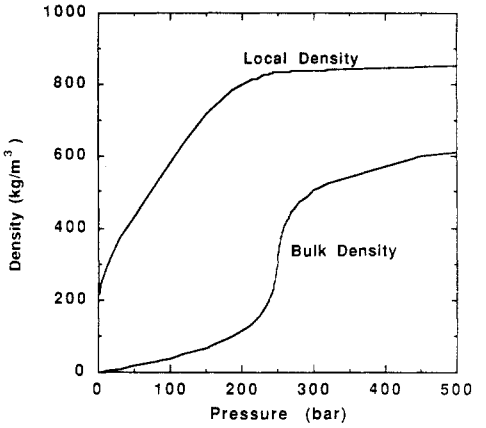

Figure 13. Comparison of bulk density with the local density 2.2 Å from the center of a univalent ion in water at 385 °C.

and the bulk density exhibit very different behavior with respect to pressure. Notice that the local density remains almost constant in the critical region where the bulk density varies greatly with pressure.

At pressures in the range between 200 and 330 bar, a very interesting physical picture emerges. The highly compressible supercritical fluid contains an ion that is surrounded by a relatively incompressible cluster, which is a condensed layer with liquidlike properties. At a slightly supercritical temperature, the fluid in the local ion environment condenses at a pressure that is far below the critical pressure. Liquidlike clusters form at low pressures, because the ion–solvent interaction, which is much stronger than the solvent–solvent interaction, condenses the solvent. An increase in the bulk pressure starting at 200 bar has little effect on the local density of this liquidlike cluster until the solvent is fully condensed. In the case of an iodide ion in water, the local density around the ion does not increase significantly until the pressure is raised above 2000 bar. At low pressures approaching zero, the local density is still much larger than the bulk density, yet this region is perhaps not of much interest, since the solubility of the ion is extremely small.

The phenomenon of clustering of a supercritical fluid solvent about a nonionic solute has been quantified from solvatochromic data obtained in the UV–visible region for various probes in pure and mixed solvents.[45–47] The ratio of the local density to the bulk density is related linearly to the isothermal compressibility, as was shown both experimentally[45] and theoretically[45,48] for fluids with low critical temperatures such as carbon dioxide, ethylene, and fluoroform. This ratio is extremely large in the highly compressible near-critical region and decreases as the compressibility decreases with pressure. In a study of [[*p*-(*N*,*N*-dimethylamino)phenyl]-ethyl]9-anthryl intramolecular exciplex fluorescence in supercritical trifluoromethane, it was found that the wavelength of the exciplex fluorescence maximum was rather insensitive to pressure.[49] The authors postulate that the probe dissolves into a cluster of solvent molecules, but that the density of this cluster does not change significantly with pressure.

The difference between the effect of clustering in absorption versus fluorescence spectroscopy may be explained as a function of the polarity of the solute in the appropriate electronic state. The process of light absorption is very fast in comparison to the speed of solvent rearrangement; therefore the degree to which the excited state is stabilized depends on the solvent environment around the unexcited molecule. As long as the ground state is relatively nonpolar, e.g. μ less than 3–5 D, the local density will be quite dependent on the bulk density in a supercritical fluid.[45] The process of exciplex fluorescence involves an excited state with

(44) Uematsu, M.; Franck, E. U. *J. Phys. Chem. Ref. Data* **1980**, *9*, 1291.

(45) Kim, S.; Johnston, K. P. *Ind. Eng. Chem. Res.* **1987**, *26*, 1206.
(46) Kim, S.; Johnston, K. P. *AIChE J.* **1987**, *33*, 1603.
(47) Yonker, C. R.; Smith, R. D. *J. Phys. Chem.* **1988**, *92*, 235.
(48) Debenedetti, P. G. *Chem. Eng. Sci.* **1987**, *42*, 2203.
(49) Okada, T.; Kobayashi, Y.; Yamasa, H.; Mataga, N. *Chem. Phys. Lett.* **1986**, *128*, 583.

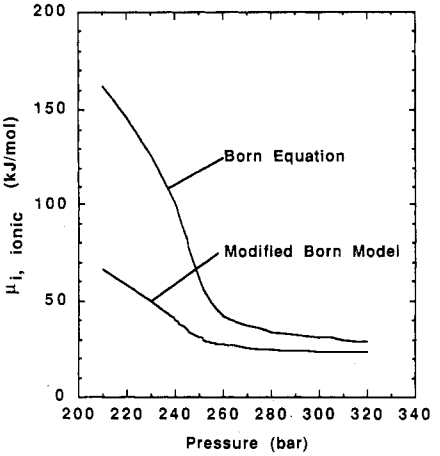

Figure 14. Free energy required to charge a 4.4-Å-diameter, univalent ion in water at 385 °C calculated with the classical Born equation, and a modified Born model that includes solvent compressibility.

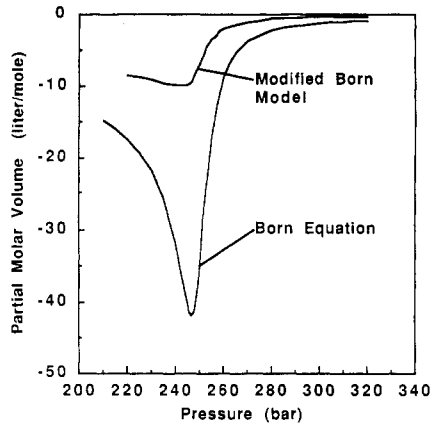

Figure 15. Partial molar volume of a 4.4-Å-diameter, univalent ion in water at 385 °C.

an extremely large dipole moment, e.g. 10 D, that persists for a period of nanoseconds, which is long enough for solvent rearrangement.[50] The modified Born model predicts that in the presence of a strong electric field, such as that near an intramolecular exciplex, the local solvent density can be much less pressure sensitive than the bulk density, as was shown in Figure 13.

The values of μ_i(ionic) predicted by the classical Born equation and the modified Born model are shown in Figure 14 for iodide ions in water at 385 °C and various pressures in the critical region. The results indicate that the increase in the local dielectric constant causes a much lower value for the calculated μ_i(ionic). The absolute values of $\bar{v}_{I^-}$(ionic) predicted by the modified Born model are much smaller than those predicted by the classical Born equation, as is shown in Figure 15, because the changes in the local density and thus the local dielectric constant are smaller than for the bulk values as a function of pressure. An equivalent statement is that clustering lowers the compressibility of the solvent near the ion (see Figure 13), which decreases the pressure effect on μ_i(ionic). This influence of clustering was also observed for a unimolecular reaction rate constant.[22]

Quint and Wood have also calculated ionic partial molar volumes, but instead of calculating $\partial\mu_i$(ionic)/∂P, they integrated the excess density around the ion.[51] The two methods are equivalent and produced the same values for a hypothetical monovalent anion.

Comparison of the Model Predictions with the Experimental Data. The calculated ionic and nonionic contributions to $\Delta\bar{v}_{rxn}$ are shown in Figure 11. The magnitude of each contribution and the total $\Delta\bar{v}_{rxn}$ are pronounced in the range where the compressibility is large and decay as the compressibility decreases (see eq 9). Although the ionic part is dominant, the nonionic contribution is significant. Between 250 and 320 bar, the average ratio of the two terms, $\Delta\bar{v}$(nonionic)/$\Delta\bar{v}$(ionic), is 0.40.

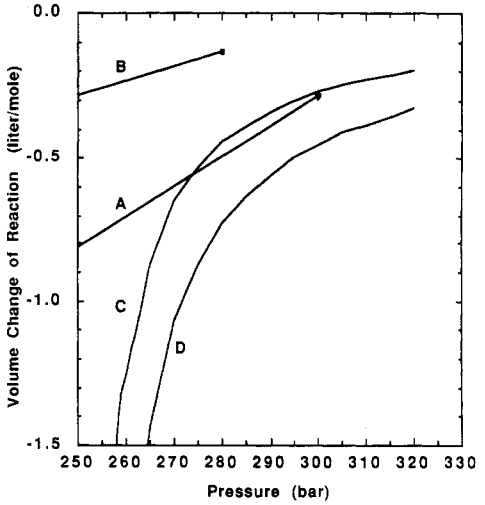

Figure 16. Comparison of the theoretical and experimental determinations of $\Delta\bar{v}_{rxn}$ for the reduction of $1/2I_2$ at 385 °C: A and B, experimentally determined upper and lower limits for $\Delta\bar{v}_{rxn}$; C, prediction of the modified Born–perturbed hard sphere model; D, prediction of the ionic modified Born portion of the model only.

The prediction of the complete model, which does not use any adjustable parameters, is compared with the experimental data in Figure 16. Above 265 bar, corresponding to $P_r \geq 1.2$, the complete theory (designated by C) predicts reasonably well the $\Delta\bar{v}_{rxn}$ and the slope of $\Delta\bar{v}_{rxn}$ with respect to pressure. These results demonstrate that it is important to include the effects of the nonionic molecular interactions as well as those of the ionic interactions. It was not possible to determine the curvature experimentally as discussed above because the fit of the potential versus pressure was limited to a quadratic expression. The curvature of the theoretical line is consistent with that of $\bar{v}_i$ of a nonpolar solute in CO_2 and that of the activation volume of α-chlorobenzyl methyl ether.[22] Each of these properties has a shape that is similar to the isothermal compressibility because of eq 9.

Below 265 bar, the model predicts much more negative values for $\Delta\bar{v}_{rxn}$ than were actually measured. The probable cause for this deviation is that the model does not address the possibility of ion pairing, which increases as the pressure and thus the dielectric constant decrease. The large increase in the solution resistance at the lower pressures provides evidence for ion pairing. Ion pairing is the first step toward the precipitation of KI or the formation of molecular HI, which will occur if the pressure is lowered much below the critical value. The electric field due to the dipole moment of an ion pair decreases as $1/r^3$, compared to $1/r^2$ for that due to an ion. Since the strength of the electrostatic forces will be smaller, the magnitude of the partial molar volume will decrease. The calculated $\Delta\bar{v}_{rxn}$ reached a minimum of −8.5 L/mol at 235 bar, which is in the region of the critical point of the mixture. It would be of interest to obtain experimental data in this region, although a great deal of effort would be required to overcome the limitation of a large solution resistance.

Conclusions

Pressure effects on electrode potentials, that is, $\Delta\bar{v}_{rxn}$'s, could be measured for the first time in supercritical water with an improved design of the electrochemical cell and microelectrodes and the extensive use of digital processing. Because of the choice of supporting electrolytes, it was possible to place limits on the effect of the thermal liquid junction potential.

It was discovered that $\Delta\bar{v}_{rxn}$ for the reduction of I_2 to I^- is extremely pronounced in the highly compressible region for the fluid. This result is consistent with partial molar volume behavior

(50) Mataga, N.; Okada, T.; Masuhara, H.; Nakashima, N. *J. Lumin.* **1976**, *12–13*, 159.
(51) Quint, J. R.; Wood, R. H. *J. Phys. Chem.* **1985**, *89*, 380.

of solutes in supercritical fluids and the activation volume for the unimolecular decomposition of α-chlorobenzyl methyl ether in 1,1-difluoroethane. The predominant contribution to $\Delta\bar{v}_{rxn}$ is the extremely large negative value of $\bar{v}_{I^-}$. The chemical potential μ_{I^-} depends on the dielectric constant, which is an extremely strong function of pressure; i.e. ϵ varies from 1.64 to 5.91 as the pressure is increased from 200 to 300 bar at 400 °C.[44] The electric field produced by the ion attracts the highly compressible water to form clusters, thus reducing the volume, as described by the modified Born model.

An analysis of clustering of a supercritical solvent about a moderately polar molecule (determined by absorption in the UV–visible region), an exciplex (determined by fluorescence), and an ion (determined by the modified Born model) leads to several important conclusions. For a given value of compressibility for the solvent, the degree of clustering increases with the strength of the solute–solvent interaction, which is related primarily to the polarity of the solute. Also, the cluster attains a liquidlike density at a lower reduced pressure as this interaction strength increases. As a result, the cluster density around a highly polar molecule is a much less sensitive function of pressure than the bulk density near the solvent critical point.

In comparison with the classic Born equation, the modified Born model predicts that the ion is more stable because of the increase in the local dielectric constant due to clustering. As a result, μ_i(ionic) is less pressure dependent, and the magnitude of $\Delta\bar{v}_{rxn}$ is smaller.

Nonionic interactions must be considered in predicting the thermodynamic properties of ionic species in supercritical fluids, even though the effects of the ionic interactions are dominant. The repulsive contribution to $\Delta\bar{v}$(nonionic), which is positive due to breaking of the I_2 bond, is much more significant than the nonionic attractive term. At pressures above 265 bar, the model predicts values of $\Delta\bar{v}_{rxn}$ that agree with the experimental values. At lower pressures, the model overpredicts the magnitude of $\Delta\bar{v}_{rxn}$, most likely because it does not consider ion pairing, which becomes prevalent. This presents an interesting challenge for future models.

Acknowledgment. We are indebted to Isaac Trachtenberg for his comments and advice concerning this research. Acknowledgment is made to the donors of the Petroleum Research Fund, administered by the American Chemical Society, the Office of Naval Research, and The University of Texas Separations Research Program for support of this research.

Appendix

To our knowledge, there are no measurements of $\partial\Delta\phi_{TLJP}/\partial P$ in the literature, although there is some information from which the sign of the derivative can be predicted for certain electrolytes. When $\partial E/\partial P$ is measured by using two different supporting electrolytes, one with positive $\partial\Delta\phi_{TLJP}/\partial P$ and one with negative $\partial\Delta\phi_{TLJP}/\partial P$, the true value of the pressure derivative will lie between the measured values.

$$\frac{\partial E}{\partial P} \text{ where } \left[\frac{\partial\Delta\phi_{TLJP}}{\partial P} \text{ is positive}\right] < \frac{\partial E_{rxn}}{\partial P} < \frac{\partial E}{\partial P} \text{ where } \left[\frac{\partial\Delta\phi_{TLJP}}{\partial P} \text{ is negative}\right] \quad \text{(A1)}$$

Prediction of the sign of $\partial\Delta\phi_{TLJP}/\partial P$ begins with an examination of some high-temperature measurements of the temperature derivative of the thermal liquid junction potential, $\partial\Delta\phi_{TLJP}/\partial T$. From the concept of the entropy of transport for an ion, introduced by Eastman,[52-54] the thermal liquid junction potential of a 1:1 electrolyte can be expressed as

$$\frac{\partial\Delta\phi_{TLJP}}{\partial T} = (t_+S_+^* - t_-S_-^*) \quad \text{(A2)}$$

where t_+ and t_- are the transference numbers of the two ions and S_+^* and S_-^* are the transport entropies of the two ions.[35,55] As an ion moves from one volume element to the next, there is an entropy change in both volumes, so the transport entropy is the difference between the entropy change in the fluid ahead of the ion and the entropy change in the fluid behind.

The quantity S^* can be expanded by using an ion in a dielectric fluid model of thermal diffusion (similar to the Born model for ion solvation)[55]

$$S^* = \frac{2q^2}{3r}\frac{\partial}{\partial T}\left(\frac{1}{\epsilon}\right) \quad \text{(A3)}$$

where q is the charge of an ion, ϵ is the dielectric constant of the fluid, and r is the radius below which the dielectric continuum assumption breaks down. The radius, r, is not explicitly defined by the theory. Macdonald et al.[35] made the assumption that neither the entropy contribution from inside of r nor the transference numbers of the ions change appreciably with temperature. This implies a linear relationship between $\partial(1/\epsilon)/\partial T$ and $(t_+S_+^* - t_-S_-^*)$. Macdonald et al. have determined $(t_+S_+^* - t_-S_-^*)$ for KCl solutions up to 250 °C and have demonstrated this linear relationship.[35]

This relationship between the dielectric constant and entropies of transport may be extended to the thermal liquid junction potential itself:

$$\frac{\partial\Delta\phi_{TLJP}}{\partial T} \approx A_1\frac{\partial}{\partial T}\left(\frac{1}{\epsilon}\right) \quad \text{(A4)}$$

where A_1 is $\{t_+(2q^2Z^2/3r_+) - t_-(2q^2Z^2/3r_-)\}$. This expression may be integrated at constant pressure to give

$$\Delta\phi_{TLJP} \approx A_1(1/\epsilon) + f(P) \quad \text{(A5)}$$

where $f(P)$ is a function of pressure that is independent of temperature. As stated above, there have been no studies of $\partial\Delta\phi_{TLJP}/\partial P$, so unfortunately there is no information available concerning the magnitude of $f(P)$. However, the molecular dynamics that give rise to the thermal liquid junction potential do not present any indication that the function is large. Therefore it will be assumed that

$$A_1(1/\epsilon) \gg f(P) \quad \text{(A6)}$$

Equation A5 may now differentiated with respect to pressure to give

$$\frac{\partial\Delta\phi_{TLJP}}{\partial P} \approx A_1\frac{\partial}{\partial P}\left(\frac{1}{\epsilon}\right) \quad \text{(A7)}$$

It is known from PVT and dielectric data for water that $\partial(1/\epsilon)/\partial T$ is always positive, while $\partial(1/\epsilon)/\partial P$ is always negative,[38,44] and therefore the sign of $\partial\Delta\phi_{TLJP}/\partial P$ is the opposite that of $\partial\Delta\phi_{TLJP}/\partial T$. This relationship is the basis for the estimation of the contribution of $\partial\Delta\phi_{TLJP}/\partial P$ to the measured changes of redox potential with pressure.

Registry No. H_2O, 7732-18-5; I^-, 20461-54-5; I_2, 7553-56-2; Pt, 7440-06-4; H_2SO_4, 7664-93-9; $KHSO_4$, 7646-93-7.

(52) Eastman, E. D. *J. Am. Chem. Soc.* **1926**, *48*, 1482.
(53) Eastman, E. D. *J. Am. Chem. Soc.* **1928**, *50*, 283.
(54) Eastman, E. D. *J. Am. Chem. Soc.* **1928**, *50*, 292.
(55) Agar, J. N. In *The Structure of Electrolyte Solutions*; Hamer, W. J., Ed.; Wiley: New York, 1959; Chapter 13.